Emerging giant resonant exciton induced by Ta substitution in anatase TiO_2: A tunable correlation effect

Z. Yong,[1,2,3,4] P. E. Trevisanutto,[2,3,5] L. Chiodo,[6,7] I. Santoso,[1,2] A. R. Barman,[2,3] T. C. Asmara,[1,2,3] S. Dhar,[1,4,14] A. Kotlov,[8] A. Terentjevs,[9] F. Della Sala,[9,10] V. Olevano,[11] M. Rübhausen,[12,13] T. Venkatesan,[1,3,4,*] and A. Rusydi[1,2,3,†]

[1]*NUSNNI-NanoCore, National University of Singapore, Singapore 117576*

[2]*Singapore Synchrotron Light Source, National University of Singapore, 5 Research Link, Singapore 117603, Singapore*

[3]*Department of Physics, National University of Singapore, Singapore 117542*

[4]*Department of Electrical and Computer Engineering, National University of Singapore, Singapore 117576*

[5]*Centre for Advanced 2D Materials and Graphene Research Centre, National University of Singapore, Singapore 117546*

[6]*Unit of Nonlinear Physics and Mathematical Modeling, Department of Engineering, Università Campus Bio-Medico di Roma, Via Álvaro del Portillo 21, 00128, Rome, Italy*

[7]*Center for Life Nano Science @Sapienza, Istituto Italiano di Tecnologia, Viale Regina Elena 291, 00161, Rome, Italy*

[8]*Photon Science at DESY, Notkestraße 85, D-22607 Hamburg, Germany*

[9]*Istituto Nanoscienze-CNR, Euromediterranean Center for Nanomaterial Modelling and Technology (ECMT), Via per Arnesano 73100 Lecce, Italy*

[10]*Center for Biomolecular Nanotechnologies @UNILE, Istituto Italiano di Tecnologia, Via Barsanti, I-73010 Arnesano, Italy*

[11]*CNRS, Institut Néel, Grenoble, France*

[12]*Institute of Nanostructure and Solid State Physics, Jungiusstrasse 11, University of Hamburg, D-20355 Hamburg, Germany*

[13]*Center for Free-Electron Laser Science, Advanced Study Group of the University of Hamburg, Luruper Chaussee 149, D-22761 Hamburg, Germany*

[14]*Department of physics, School of Natural Sciences, Shiv Nadar University, Gautam Buddha Nagar, P.O. NH-91, Uttar Pradesh 201314, India*

(Received 7 June 2015; revised manuscript received 26 March 2016; published 12 May 2016)

Titanium dioxide (TiO_2) has rich physical properties with potential implications for both fundamental physics and new applications. To date, the main focus of applied research is to tune its optical properties, which is usually done via doping and/or nanoengineering. However, understanding the role of d electrons in materials and possible functionalization of d-electron properties are still major challenges. Herewith, within a combination of an innovative experimental technique, high-energy optical conductivity, and state-of-the-art *ab initio* electronic structure calculations, we report an emerging, novel resonant exciton in the deep ultraviolet region of the optical response. The resonant exciton evolves upon low-concentration Ta substitution in anatase TiO_2 films. It is surprisingly robust and related to strong electron-electron and electron-hole interactions. The d- and f-orbital localization, due to Ta substitution, plays an unexpected role, activating strong electronic correlations and dominating the optical response under photoexcitation. Our results shed light on a new optical phenomenon in anatase TiO_2 films and on the possibility of tuning electronic properties by Ta substitution.

DOI: 10.1103/PhysRevB.93.205118

I. INTRODUCTION

Doped or defective titanium dioxide (TiO_2) exhibits rich physical phenomena in electronic transport and optical properties [1–4]. TiO_2 is opaque in visible sunlight, whereas it is very efficient at absorbing ultraviolet (UV) light, rendering it interesting especially for photocatalysis applications [5]. The first step in photoexcitation is the formation of electron-hole pair quasiparticles (excitons), which may either recombine or decay into free charges. Eventually the free charges react with molecules on the surface, enhancing photocatalytic effects and formation of reactive free radicals [6]. Excitons, and their spatial behavior, therefore play a key role in both fundamental physics and applications, but the precise nature and behavior of excitons in TiO_2-based materials remains unclear in some respects.

Many-body electron-electron (e-e) and electron-hole (e-h) interactions determine the physical properties of excitons, with different contributions, depending on the system and on the considered energy range. Excitons usually occur below the direct band gap in semiconductor and insulator materials, but they may involve higher energy bands in the case of a strong electronic correlation. With the recent development of supercomputing and *ab initio* calculations [7–9], theoretical studies have shown that when both e-e and e-h interactions are strongly coupled, they yield to a new type of optical phenomenon, the so-called high-energy resonant excitonic effect. In fact, resonant excitons have been predicted [10,11] and later observed [12,13] in two-dimensional graphene. Unlike excitons in conventional semiconductors, the resonant excitons can occur at energies even well above the corresponding optical band gap of the material, and they can be probed directly using high-energy optical conductivity [13]. A detailed understanding of the role of e-e and e-h interactions in TiO_2-based materials remains elusive, and resonant excitons have not been observed in the material, mainly because both

*venky@nus.edu.sg
†phyandri@nus.edu.sg

experimental and theoretical studies at a high-energy optical conductivity are challenging and limited in number.

We report in this paper on optical studies of TiO_2 doped at different concentrations of tantalum, via optical conductivity measurements and *ab initio* time-dependent density functional theory (TDDFT) calculations. We have observed resonant excitonic effects in the deep ultraviolet in anatase $Ta_x\ Ti_{1-x}O_2$ films, with only a small amount of Ta substitution. A series of unusual phenomena arises, in particular, the spectral-weight transfer from high towards low energies and the emergence of an intense resonant exciton at ∼6 eV. Based on our theoretical calculations, we relate these effects to a peculiar manifestation of strong e-e and e-h interactions. The paper is organized as follows: in Sec. II, experimental and theoretical-computational techniques used are described. In Sec. III, optical spectra, both measured and calculated, are described. In Sec. IV, the main conclusions are drawn.

II. MATERIALS AND METHODS

Details of sample preparation and characterization, optical conductivity measurements, and theoretical calculations are described in this section.

A. Experimental techniques

The optical conductivity was obtained using a combination of spectroscopic ellipsometry (0.5- to 5.6-eV) and UV-VUV reflectivity (3.7- to 35-eV) measurements [14,15]. The spectroscopic ellipsometry measurements were performed in the spectral range between 0.5 and 5.6 eV by using an SE 850 ellipsometer at room temperature. Three incidence angles, 60°, 70°, and 80° from the sample normal were used, and the incident light was 45° linearly polarized from the plane of incidence. For reflectivity measurements in the high-energy range between 3.7 and 35 eV, we used the SUPERLUMI beamline at the DORIS storage ring of HASYLAB (DESY) [16]. The incoming photon was incident at an angle of 17.5° from the sample normal, with linear polarization parallel to the sample surface. The sample chamber was outfitted with a gold mesh to measure the incident photon flux after the slit of the monochromator. The measurements were performed in an ultrahigh-vacuum environment (chamber pressure of 5×10^{-10} mb) at room temperature. Before these measurements, the samples were heated up to 400 K in an ultrahigh vacuum to ensure that there were no additional adsorbate layers on the surface of the samples. The obtained UV-VUV reflectivity data were calibrated by comparison with the luminescence yield of sodium salicylate ($NaC_7H_5O_3$) and the gold-mesh current. These as-measured UV-VUV reflectivity data were further normalized by using the self-normalized reflectivity extracted from spectroscopic ellipsometry [15,17].

B. Experimental samples and preparations

Ta_2O_5 and TiO_2 powders of a high purity (99.999%) were ground for several hours before sintering in a furnace at 1000°C in air for 20 h. Subsequently, target pellets were made and sintered at 1100°C in air for 24 h. Anatase $Ta_xTi_{1-x}O_2$ epitaxial thin films (with $x = 0$, 0.018, and 0.038) of thickness 280 nm were deposited on high-quality (001) $LaAlO_3$ substrates by pulsed laser deposition, using a 248-nm Lambda Physik excimer laser with an energy density of 1.8 J cm^{-2} and a repetition rate of 2–10 Hz. Depositions were performed for 0.51 h at a stable oxygen partial pressure of 1×10^{-5} Torr, while the substrate temperature was maintained at 750°C. The chemical and structural properties of the samples were studied by x-ray photoemission spectroscopy, electrical transport measurements, Rutherford backscattering spectrometry/channeling, x-ray diffraction, and time-of-flight secondary-ion mass spectrometry as reported elsewhere [18,19]. Ion channeling measurements indicated near-perfect substitutional Ta atoms in Ti sites.

C. Theoretical and computational methods

All ground-state electronic calculations are carried out using density functional theory (DFT) based on the QUANTUM ESPRESSO [20] and ABINIT [21] codes, with the Perdew-Burke-Ernzerhof (PBE)-GGA approximation for the exchange-correlation functional [22]. Norm-conserving pseudopotentials in Troullier-Martins scheme [23] are used, and semicore electrons are included in Ti and Ta pseudopotentials. The cutoff energy for the expansion of the plane-wave basis is up to 170 Ry [24]. For pristine anatase TiO_2, we used a $12 \times 12 \times 8$ Monkhorst-Pack k-point mesh sampling the Brillouin zone. For anatase Ta-TiO_2 bulk we used supercells with 48 atoms and a $4 \times 4 \times 4$ Monkhorst-Pack k-point mesh grid. One Ti atom is replaced with one Ta atom [substitutional doping, modeling a 6.5% Ta doping in TiO_2 bulk, almost equivalent to the experimental doped sample (3.8%)].

Excited-state calculations are performed within two approaches: solving the Bethe Salpeter Equation [(BSE), which implicitly includes both e-h and e-e interactions], and applying the jellium-with-gap model (JGM) kernel [25] within the TDDFT. The latter method includes the e-e and e-h interactions maintaining the computational feasibility for such complex calculations. The complex dielectric function has also been evaluated at the random phase approximation (RPA) level, with electrons and holes treated as independent particles, without correlation. The BSE has been solved using YAMBO code [26] and EXC [27]. The screening dieletric matrix has been evaluated by using the static inverse dielectric function, with cutoffs of 21 Ry for the correlation (exchange) part, and unoccupied states are summed over 176 empty states. In BSE calculations defined hereafter as low resolution (LR), 28 occupied bands and 52 empty bands are included in the diagonalization, to describe the region above 5 eV, on a k-point grid of $4 \times 4 \times 2$. For the high-resolution (HR) BSE calculation, used to describe the adsorption threshold in more detail, 8 occupied and 8 empty bands are included in the diagonalization, on a $12 \times 12 \times 12$ k-point grid. The Haydock recursive approach for diagonalization is used, with a threshold accuracy of −0.02. The DP-EXC code [28] is used for TDDFT calculations. In pristine bulk TiO_2, 200 bands are included for the RPA and JGM-TDDFT calculations.

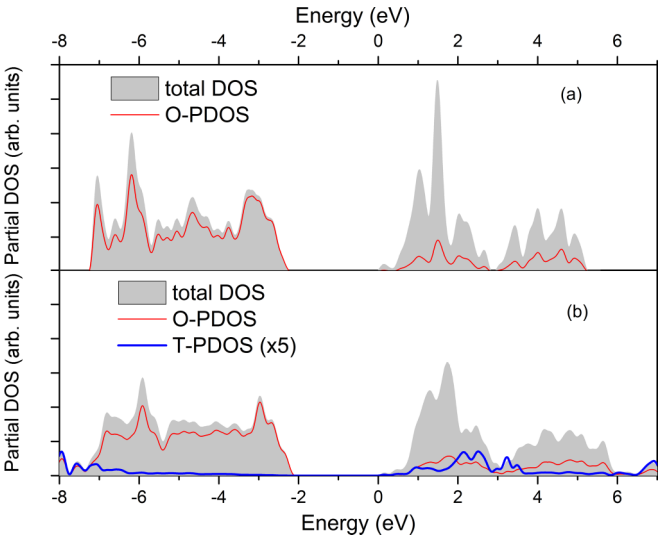

FIG. 1. (a) Total DOS of anatase TiO_2 from DFT calculations. The black line represents the total DOS; the red line, the oxygen partial DOS. (b) DOS of 6.5 % Ta-substituted anatase TiO_2. The blue line is the partial DOS of the Ta atom multiplied by a factor of 5 to make the peak positions clearer.

III. RESULTS AND DISCUSSION

A. Energy levels of TiO_2 and Ta-TiO_2

Here, we provide some general information on pure TiO_2, useful in the following discussion on optical conductivity. The electronic ground-state structure of pristine and doped TiO_2, based on DFT results for the total density of states (DOS) and partial DOS (PDOS), is shown in Fig. 1. The DFT-PBE band gap of pristine TiO_2 is ~2.20 eV. The valence band [Fig. 1(a)] mainly consists of O 2*p* orbitals slightly hybridized with Ti 3*d* orbitals. The conduction band is comprised of Ti 3*d* orbitals with a small hybridized number of O 2*p* orbitals.

In Ta-TiO_2 [Fig. 1(b)], the 3*d* Ta orbitals fill the bottom of the conduction band, making the system metallic, and they are hybridized with the adjacent O 2*p* orbitals up to 8 eV in the conduction band. The proper inclusion of the correlation removes this spurious metallicity described by DFT, as shown for Nb-doped rutile [29]. The main features of the electronic band structure [Fig. 2(a)] and optical absorption spectrum of anatase TiO_2 have been studied for a long time, and they have been thoroughly revised and reanalyzed recently [30].

B. Optical properties of Ta-TiO_2

Next, we focus on the large spectral changes induced by Ta doping in the optical response, even for small amounts of Ta substitution. Figure 3 shows the optical conductivity of TiO_2 and Ta-doped TiO_2 films, at increasing Ta doping and in a broad energy range, up to ~35 eV. Ta_x $Ti_{1-x}O_2$ films are measured for $x = 0$, 0.018, and 0.038. For $x = 0$, the pure TiO_2 sample, we observe first sharp optical excitation at 3.48 eV (P1; see inset in Fig. 3), followed by bulk resonances from 3.85 to 4.6 eV (P2) [30]. A well-defined large peak, at ~6.12 eV (P3), is a newly observed intense bulk resonance in pure TiO_2. It is followed by broad and multiple structures up to ~35 eV.

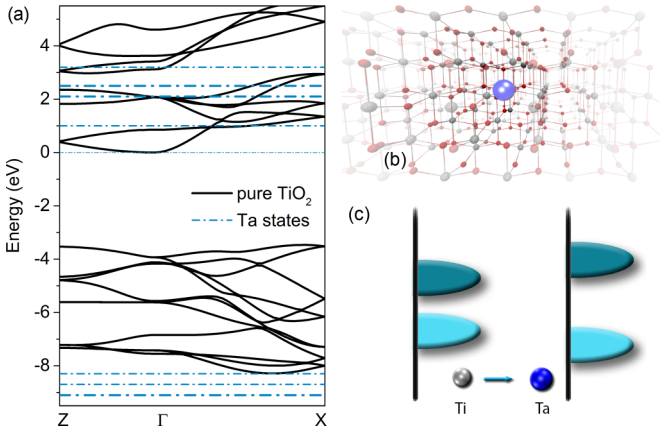

FIG. 2. (a) Anatase band structure (black line) along the high-symmetry directions Z-Γ-X of the Brillouin zone. A scissor of 1.2 eV has been applied on top of the PBE-DFT band structure. Ta-derived states, extrapolated from the PDOS analysis, have been superimposed on the pristine TiO_2 band structure (dashed blue line). We can rule out a direct effect of Ta doping on optical properties, as neither do optical transitions involving Ta states coincide in energy with peaks observed in optical conductivity nor could the PDOS associated with the low Ta doping considered here generate the intense optical features we observed. (b) Graphical representation of the long-range correlation effects of the low Ta doping in TiO_2 anatase crystals. (c) A simplified cartoon representation of the effects of Ti-Ta substitution that turns on the on-site Coulomb repulsion involving *d*-Ti and *p*-O states. The on-site repulsive interaction induces a band-gap opening, giving optical transitions above the optical gap.

Upon Ta substitution ($x = 0.018$) we observe an emerging new giant peak at 6.0 eV (E2; Fig. 3), three times more intense than the P3 peak of pure anatase. At 6.8 eV there is an intense shoulder (E3) of the giant peak E2. The first optical excitation is also affected by Ta doping, as it occurs at a higher energy

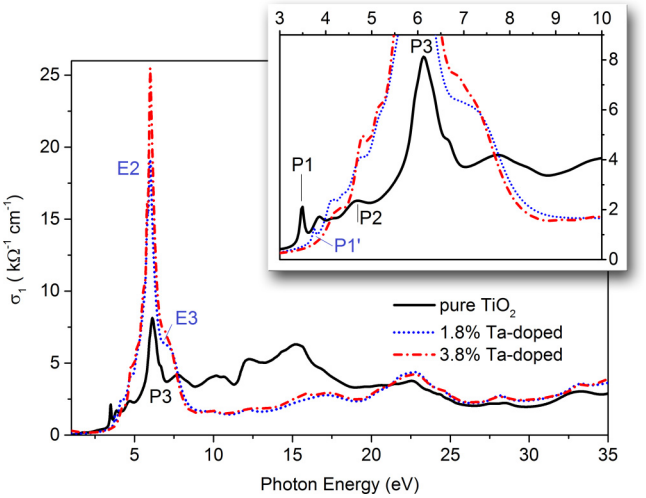

FIG. 3. Room-temperature measurements of the real part of the optical conductivity for pure TiO_2 (solid black line), 1.8% (short blue dotted line), and 3.8% Ta-substituted TiO_2 (red dashed-dotted line). The polarization vector is perpendicular to the [001] direction. Inset: Details of the real part of the optical conductivity in the VIS and low-UV regions.

(3.75 eV, P1′ ≡ E_1) and reduced intensity with respect to the pure sample. Furthermore, upon substitutional doping, the spectrum shows a significant reduction in the spectral weight in a broad energy range (from ∼8 to ∼20 eV) and a slight spectral-weight gain, singular at even a higher energy (from ∼20 to ∼35.0 eV). For a higher Ta concentration ($x = 0.038$), the E2 peak at 6.0 eV shows a further enhanced intensity, without any significant change in the remaining structures with respect to the lower Ta concentration. To summarize, we have, upon Ta doping, (i) an anomalous spectral-weight transfer from energies as high as 35 eV towards the 6-eV region; (ii) the emergence of a novel resonant exciton, E2, at 6 eV; and (iii) the strong modification of TiO_2 optical conductivity, with an augmented optical band gap. The optical conductivity here measured in such a broad energy range proves crucial to investigation of the nature of E2. Based on the optical f-sum rule, we find that the total spectral weight (up to 35 eV) is nearly conserved for all three investigated doping ratios (Fig. 3). This directly implies that the oscillator strength at 6.0 eV comes from spectral-weight transfers of the higher bands, i.e., from 8 to 20 eV. Such a collective spectral-weight transfer is a fingerprint of strong electronic correlations [31–33]. Our theoretical analysis (see below) shows that the E3 peak in Ta_x $Ti_{1-x}O_2$ has an origin similar to that of the P3 peak at 6.12 eV in undoped TiO_2, while E2 can be associated with an evolution of the bulk resonance P2. Further, based on our theoretical calculations, we could investigate the role of e-e and e-h interactions, clarifying the nature of the giant exciton E2 and confirming that the observed optical behavior is due to a manifestation of strong e-e and e-h interactions.

C. Theoretical results

In Fig. 4(a), we show the optical conductivity of pure TiO_2 calculated using the three above-mentioned theoretical methods. GW-BSE calculations, taking into account both e-e and e-h interactions, give rise to bound and resonant excitons or other excitonic effects along with spectral-weight transfers. The comparison between GW-BSE and GW-RPA results therefore gives a direct measure of the excitonic nature of a resonance. The GW-RPA calculation fails to reproduce the P2 bulk resonance and the structures near the absorption edges, while both the GW-BSE and the JGM-TDDFT, with some differences in their details, are able to describe the P1 and P2 peaks. This confirms that the e-e and e-h interactions are significant and important, not only for doped anatase, but even for pure TiO_2, in agreement with previous results [24,34]. We plot here the optical conductivity, but we note that our GW-BSE result (HR) for optical absorption (not shown) is comparable to previous calculations for the TiO_2 dielectric function [12,13,30,31]. From Refs. [24] and [30], we know that the P1 peak (experimentally at ∼3.48 eV) is related to the bound exciton, whereas P2 (at ∼4.6 eV) comes from a bulk resonance.

The LR and HR GW-BSE data allow us to properly align and identify the JGM-TDDFT spectral features with respect to experimental data, having as reference the P2 peak. The JGM-TDDFT and HR-GW-BSE coincide in intensity and energy for the P2 peak, whereas for the P3 peak and higher energy features, LR-GW-BSE calculations are in good agreement with the JGM-TDDFT. Upon Ta substitution, the solution of the GW-BSE becomes computationally cumbersome. We turn therefore to the JGM-TDDFT, which is equally reliable, as just shown in the case of pure TiO_2 but computationally feasible also for large supercells.

We focus on optical features in the region of ∼6.0 eV, and we use TDDFT to qualitatively study the relationship between E_g (and therefore the screening properties of the material) and resonant excitonic effects in Ta_x $Ti_{1-x}O_2$. In Fig. 4(b), we show JGM-TDDFT results for increasing band-gap values, $E_g = 3.2$, 3.5, and 3.7 eV for Ta_x $Ti_{1-x}O_2$. The strong correlation mimicked by E_g is reflected in the optical response, in particular, in the behavior of the peak at 6.0 eV. Peak P2 undergoes a red shift of almost 1 eV, and at the same time its intensity increases. Other features in the spectrum (as P3) undergo a similar shift, but no intensity changes are observed other than for P2.

In Fig. 5(a), we compare the experimental findings with the theoretical calculations. Even though the results differ in intensity, both P2 and P3 are present. Nevertheless, when the JGM-TDDFT with $E_g = 3.7$ eV is compared with the Ta-TiO_2 optical conductivity [Fig. 5(b)], the theoretical calculations qualitatively suggest that peak P2 is evolving in the E2 exciton at 6.0 eV, whereas the P3 peak at ∼6.1 eV is transforming in the shoulder E3 at 6.8 eV [Fig. 5(b)]. This seems to be counterintuitive looking at only the experimental optical conductivity results for pure and Ta-substituted TiO_2 but becomes clear when the proper alignment and assignment of optical features are performed. From the current results, it

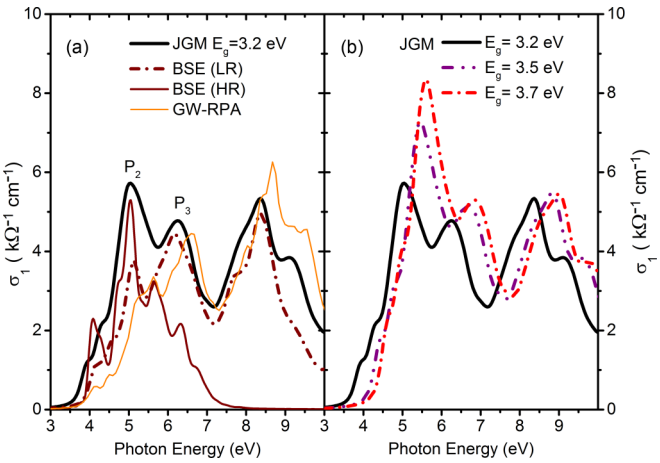

FIG. 4. (a) Calculated optical conductivity ([001] in-plane polarization) for anatase TiO_2 in the GW-RPA approximation (solid orange line), solving the Bethe-Salpeter equation in a low-resolution (LR-BSE; dark-red dashed-dotted line) and a high-resolution BSE (HR-BSE; dark-red solid line), and within TDDFT using the JGM kernel with $E_g = 3.2$ eV − experimental indirect band gap of TiO_2 (solid black line). HR-BSE calculations include more stringent convergence parameters, but with fewer included conduction bands. LR-BSE calculations are performed to describe high-energy features (beyond 6 eV). Both of them are performed to validate the JGM-TDDFT calculations. (b) Optical conductivity ([001] in-plane polarization) for anatase Ta_x $Ti_{1-x}O_2$ calculated by TD-DFT with the JGM kernel and an E_g of 3.2 eV (solid black line), 3.5 eV (dotted purple line), and 3.7 eV (dashed-dotted red line). Increasing E_g results in an enhanced peak at 6 eV.

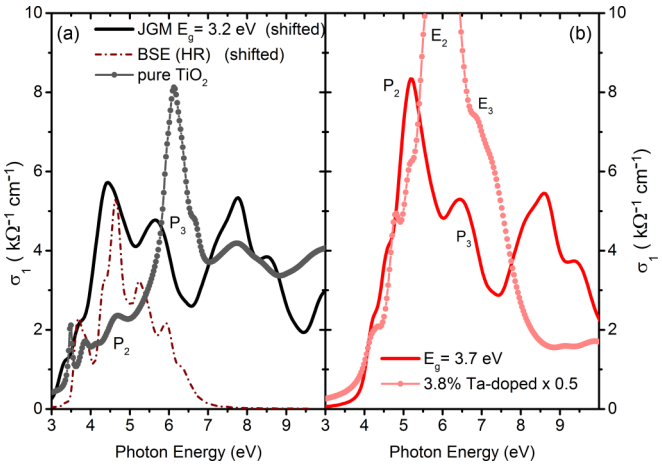

FIG. 5. (a) Comparison between experimental (solid gray line with circles) and BSE (dark-red dot-dashed line) and JGM-TDDFT ($E_g = 3.2$ eV; solid black line). Optical conductivity calculations for pure anatase TiO_2. A rigid shift of -0.6 eV has been applied to align the theoretical spectra with the experimental data. (b) Experimental optical conductivity (pink circles) and JGM-TDDFT calculations (solid red line) for Ta-substituted (3.8% TiO_2 with $E_g = 3.7$ eV). A rigid shift of -0.6 eV has been applied to align the theoretical spectra with experimental data.

seems that E2, evolving from P2, is indeed a resonant exciton emerging from an electron-hole continuum which exists at higher energy bands, well beyond a continuum spectrum.

D. Strong correlations

Our JGM-TDDFT calculations display an interplay between E_g and the resonant excitons, i.e., a larger E_g reflects an enhancement of the resonant excitonic effects. Furthermore, the JGM-TDDFT calculations support the following scenario: the resonant exciton E2 at $\sim$6 eV in the experimental spectra can be related to a modification of the electronic structure under Ta substitution, leading also to the opening of the band gap. This result is in contrast to blue the conventional picture, where Ta substitution would lead to a simple electron doping and metallization of TiO_2. In fact, our findings imply that Ta substitution in Ta_x $Ti_{1-x}O_2$ does not act as a conventional dopant but, instead, plays an unusual role in enhancing strong electronic correlations. A behavior showing some similarities to these results has recently been reported for a magnetic-doped TiO_2 system. Theoretical investigation of magnetic Cr-doped TiO_2 [35] shows that upon Cr doping the electronic properties undergo a transformation, and the (initially charge transfer insulator) system becomes a strongly correlated Mott-Hubbard crystal. We observe here an optical response which is the consequence of a similar effect in the electronic structure: the excitonic strength results in an enhancement of the absorption peak upon band-gap opening. Upon electron doping via Ta substitution, a possible scenario to describe the increasing electronic correlation involves the Ti d-d and Ti d-O p orbital repulsions, but a more detailed analysis is left to frameworks with a better treatment of strongly correlated interactions. The scenario for Ta-doped TiO_2 optics presents conceptual similarities to that for strongly correlated materials, such as cuprates like doped $La_{2-x}Sr_xCuO_4$ [36,37]. In this respect, TiO_2 is widely considered an intermediate oxide between the charge transfer insulator and Mott-Hubbard regimes [38,39]. We observe some analogies between our Ta-doped semiconductor spectra and the optical behavior of undoped Mott insulators (as cuprates), where intense optical absorption in the deep ultraviolet is due to transitions from the lower to the upper Hubbard band. In the case of Mott insulators, the change in E_g (or the Mott gap [34]) as a function of doping gives a signature of the e-e correlation. Using the DMFT, it has been shown that different percentages of doping induce a change of phase. The increase in d states modifies their electronic DOS, and the pseudogap material becomes insulating. This results in a strong enhancement of peak intensities in the optical conductivity. A similar behavior may be revealed in the present case where the inclusion of Ta d and f orbitals seem to have a role in changing the TiO_2 physics, increasing both e-e and e-h correlations.

IV. CONCLUSIONS

In conclusion, we have presented the emergence of an intense resonant exciton induced by Ta substitution in anatase TiO_2. This result is of primary importance for possible industrial applications. We argue that these experimental findings show that tunable e-e and e-h correlations play a key role in the observed resonant excitons in the Ta_x $Ti_{1-x}O_2$ system and can be used in a model for resonant excitonic effects. Further works will be devoted to improve our qualitative description in a more quantitative agreement with the experimental results.

ACKNOWLEDGMENTS

This work was supported by Singapore National Research Foundation under its Competitive Research Funding (NRF-CRP 8-2011-06), MOE-AcRF Tier-2 (MOE2015-T2-1-099), FRC (R-144-000-368-112), the 2015 PHC Merlion Project, and BMBF 05K14GUB. We acknowledge the CSE-NUS computing center, Centre for Advanced 2D Materials, and Graphene Research Centre for providing facilities for our numerical calculations. We also acknowledge the National Research Foundation, Prime Minister Office, Singapore, under its Medium Sized Centre Programme and Competitive Research Funding (R-144-000-295-281). L.C. acknowledges M. Lauricella and J. Sofo for useful discussions. The authors acknowledge F. Da Pieve for a critical reading of the manuscript.

Z.Y., P.E.T., and L.C. contributed equally to this article.

[1] O. Dulub *et al.*, Electron-induced oxygen desorption from the TiO_2(011)-2×1 surface leads to self-organized vacancies, Science **317**, 1052 (2007).

[2] E. J. W. Crossland *et al.*, Mesoporous TiO_2 single crystals delivering enhanced mobility and optoelectronic device performance, Nature **495**, 215 (2013).

[3] C. Richter and C. A. Schmuttenmaer, Exciton-like trap states limit electron mobility in TiO_2 nanotubes, Nat. Nanotechnol. **5**, 769 (2010).

[4] B. O'Regan and M. Grätzel, A low-cost, high-efficiency solar cell based on dye-sensitized colloidal TiO_2 films, Nature **353**, 737 (1991).

[5] I. Chung, B. Lee, J. He, R. P. H. Chang, and M. G. Kanatzidis, All-solid-state dye-sensitized solar cells with high efficiency, Nature **485**, 486 (2012).

[6] E. W. McFarland and J. Tang, A photovoltaic device structure based on internal electron emission, Nature **421**, 616 (2003).

[7] S. Albrecht, L. Reining, R. Del Sole, and G. Onida, *Ab initio* Calculation of Excitonic Effects in the Optical Spectra of Semiconductors, Phys. Rev. Lett. **80**, 4510 (1998).

[8] L. X. Benedict, E. L. Shirley, and R. B. Bohn, Optical Absorption of Insulators and the Electron-Hole Interaction: An *ab initio* Calculation, Phys. Rev. Lett. **80**, 4514 (1998).

[9] M. Rohlfing and S. G. Louie, Electron-Hole Excitations in Semiconductors and Insulators, Phys. Rev. Lett. **81**, 2312 (1998).

[10] L. Yang, J. Deslippe, C.-H. Park, M. L. Cohen, and S. G. Louie, Excitonic Effects on the Optical Response of Graphene and Bilayer Graphene, Phys. Rev. Lett. **103**, 186802 (2009).

[11] P. E. Trevisanutto, M. Holzmann, M. Côté, and V. Olevano, *Ab initio* high-energy excitonic effects in graphite and graphene, Phys. Rev. B **81**, 121405(R) (2010).

[12] K. F. Mak, J. Shan, and T. F. Heinz, Seeing Many-Body Effects in Single- and Few-Layer Graphene: Observation of Two-Dimensional Saddle-Point Excitons, Phys. Rev. Lett. **106**, 046401 (2011).

[13] I. Santoso, P. K. Gogoi, H. B. Su, H. Huang, Y. Lu, D. Qi, W. Chen, M. A. Majidi, Y. P. Feng, A. T. S. Wee, K. P. Loh, T. Venkatesan, R. P. Saichu, A. Goos, A. Kotlov, M. Rübhausen, and A. Rusydi, Observation of room-temperature high-energy resonant excitonic effects in graphene, Phys. Rev. B **84**, 081403(R) (2011).

[14] A. Rusydi, R. Rauer, G. Neuber, M. Bastjan, I. Mahns, S. Müller, P. Saichu, B. Schulz, S. G. Singer, A. I. Lichtenstein, D. Qi, X. Gao, X. Yu, A. T. S. Wee, G. Stryganyuk, K. Dörr, G. A. Sawatzky, S. L. Cooper, and M. Rübhausen, Metal-insulator transition in manganites: Changes in optical conductivity up to 22 eV, Phys. Rev. B **78**, 125110 (2008).

[15] T. C. Asmara *et al.*, Mechanisms of charge transfer and redistribution in $LaAlO_3/SrTiO_3$ revealed by high-energy optical conductivity, Nat. Commun. **5**, 3663 (2014).

[16] G. Zimmerer, Status report on luminescence investigations with synchrotron radiation at HASYLAB, Nucl. Instrum. Methods Phys. Res. A **308**, 178 (1991).

[17] T. C. Asmara, I. Santoso, and A. Rusydi, Self-consistent iteration procedure in analyzing reflectivity and spectroscopic ellipsometry data of multilayered materials and their interfaces, Rev. Sci. Instrum. **85**, 123116 (2014).

[18] A. Rusydi *et al.*, Cationic-vacancy-induced room-temperature ferromagnetism in transparent, conducting anatase $Ti_{1x}Ta_xO_2(x0.05)$ thin films, Philos. Trans. Roy. Soc. London A: Math. Phys. Eng. Sci. **370**, 4927 (2012).

[19] D.-C. Qi, A. R. Barman, L. Debbichi, S. Dhar, I. Santoso, T. C. Asmara, H. Omer, K. Yang, P. Krüger, A. T. S. Wee, T. Venkatesan, and A. Rusydi, Cationic vacancies and anomalous spectral-weight transfer in $Ti_{1x}Ta_xO_2$ thin films studied via polarization-dependent near-edge x-ray absorption fine structure spectroscopy, Phys. Rev. B **87**, 245201 (2013).

[20] P. Giannozzi *et al.*, QUANTUM ESPRESSO: A modular and open-source software project for quantum simulations of materials, J. Phys. Condens. Matter **21**, 395502 (2009).

[21] X. Gonze *et al.*, ABINIT: First-principles approach to material and nanosystem properties, Comput. Phys. Commun. **180**, 2582 (2009).

[22] J. P. Perdew, K. Burke, and M. Ernzerhof, Generalized Gradient Approximation Made Simple, Phys. Rev. Lett. **77**, 3865 (1996).

[23] N. Troullier and J. L. Martins, Efficient pseudopotentials for plane-wave calculations. 2. Operators for fast iterative diagonalization, Phys. Rev. B **43**, 8861 (1991).

[24] L. Chiodo *et al.*, Self-energy and excitonic effects in the electronic and optical properties of TiO_2 crystalline phases, Phys. Rev. B **82**, 045207 (2010).

[25] P. E. Trevisanutto, A. Terentjevs, L. A. Constantin, V. Olevano, and F. D. Sala, Optical spectra of solids obtained by time-dependent density functional theory with the jellium-with-gap-model exchange-correlation kernel, Phys. Rev. B **87**, 205143 (2013).

[26] A. Marini, C. Hogan, M. Grüning, and D. Varsano, YAMBO: An *ab initio* tool for excited state calculations, Comput. Phys. Commun. **180**, 1392 (2009).

[27] http://www.bethe-salpeter.org.

[28] http://www.dp-code.org.

[29] M. Zhang, S. Ono, and K. Ohno, All-electron GW calculation of rutile TiO_2 with and without Nb impurities, Phys. Rev. B **92**, 035205 (2015).

[30] E. Baldini, L. Chiodo, A. Dominguez, M. Palummo, S. Moser, M. Yazdi, G. Aubock, B. P. P. Mallett, H. Berger, A. Magrez, C. Bernhard, M. Grioni, A. Rubio, and M. Chergui, Two-dimensional excitonic quasiparticles in a three-dimensional crystal: The case of anatase TiO_2, arXiv:1601.01244 [cond-mat].

[31] H. Eskes, M. B. J. Meinders, and G. A. Sawatzky, Anomalous Transfer of Spectral Weight in Doped Strongly Correlated Systems, Phys. Rev. Lett. **67**, 1035 (1991).

[32] Y. Ohta, K. Tsutsui, W. Koshibae, T. Shimozato, and S. Maekawa, Evolution of the in-gap state in high-Tc cuprates, Phys. Rev. B **46**, 14022 (1992).

[33] P. Phillips, Colloquium: Identifying the propagating charge modes in doped Mott insulators, Rev. Mod. Phys. **82**, 1719 (2010).

[34] W. Kang and M. S. Hybertsen, Quasiparticle and optical properties of rutile and anatase TiO_2, Phys. Rev. B **82**, 085203 (2010).

[35] F. Da Pieve, S. Di Matteo, T. Rangel, M. Giantomassi, D. Lamoen, G.-M. Rignanese, and X. Gonze, Origin of Magnetism and Quasiparticles Properties in Cr-Doped TiO_2, Phys. Rev. Lett. **110**, 136402 (2013).

[36] T. Das, R. S. Markiewicz, and A. Bansil, Strong correlation effects and optical conductivity in electron-doped cuprates, Eur. Phys. Lett. **96**, 27004 (2011).

[37] C. Weber, K. Haule, and G. Kotliar, Optical weights and waterfalls in doped charge-transfer insulators: A local

density approximation and dynamical mean-field theory study of $La_{2x}Sr_xCuO_4$, Phys. Rev. B **78**, 134519 (2008).

[38] J. Zaanen, G. A. Sawatzky and, J. W. Allen, Band Gaps and Electronic Structure of Transition-Metal Compounds, Phys. Rev. Lett. **55**, 418 (1985).

[39] A. E. Bocquet, T. Mizokawa, K. Morikawa, A. Fujimori, S. R. Barman, K. Maiti, D. D. Sarma, Y. Tokura, and M. Onoda, Electronic structure of early 3*d*-transition-metal oxides by analysis of the 2*p* core-level photoemission spectra, Phys. Rev. B **53**, 1161 (1996).